

AUGUST 2016

M.Sc. in Mechanical Engineering

ÖMER ÖZDEN KESKİN

UNIVERSITY OF GAZİANTEP
GRADUATE SCHOOL OF
NATURAL & APPLIED SCIENCES

**INVESTIGATION OF CYLINDRICAL PART MANUFACTURING BY
SHAPED METAL DEPOSITION**

M.Sc. THESIS

IN

MECHANICAL ENGINEERING

BY

ÖMER ÖZDEN KESKİN

AUGUST 2016

**Investigation of Cylindrical Part
Manufacturing by Shaped Metal Deposition**

**M.Sc. Thesis
in
Mechanical Engineering
University of Gaziantep**

**Supervisor
Assoc. Prof. Dr. Oğuzhan YILMAZ**

**by
Ömer Özden KESKİN**

August 2016



© 2016 [Ömer Özden KESKİN]

REPUBLIC OF TURKEY
UNIVERSITY OF GAZİANTEP
GRADUATE SCHOOL OF NATURAL & APPLIED SCIENCES
MECHANICAL ENGINEERING

Name of the thesis: Investigation of Cylindrical Part Manufacturing by Shaped Metal Deposition

Name of the student: Ömer Özden KESKİN

Exam date: 03.08.2016

Approval of the Graduate School of Natural and Applied Sciences


Prof. Dr. Metin BEDİR

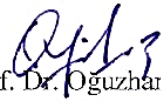
Director

I certify that this thesis satisfies all the requirements as a thesis for the degree of Master of Science.


Prof. Dr. Mehmet Saif SOYLEMEZ

Head of Department

This is to certify that we have read this thesis and that in our consensus/majority opinion it is fully adequate, in scope and quality, as a thesis for the degree of Master of Science.


Assoc. Prof. Dr. Oguzhan YILMAZ

Supervisor

Examining Committee Members:

Prof. Dr. Rahmi ÜNAL

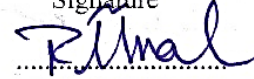
Prof. Dr. Ömer EYERCİOĞLU

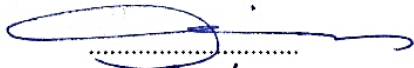
Assoc. Prof. Dr. Oguzhan YILMAZ

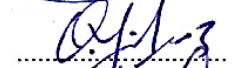
Assoc. Prof. Dr. Yusuf USTA

Assist. Prof. Dr. A.Tolga BOZDANA


Signature











I hereby declare that all information in this document has been obtained and presented in accordance with academic rules and ethical conduct. I also declare that, as required by these rules and conduct, I have fully cited and referenced all material and results that are not original to this work.

Ömer Özden KESKİN

ABSTRACT
INVESTIGATION OF CYLINDRICAL PART
MANUFACTURING BY SHAPED METAL DEPOSITION

KESKİN, Ömer Özden

M.Sc. in Mechanical Engineering

Supervisor: Assoc. Prof. Dr. Oğuzhan YILMAZ

August 2016

57 Pages

Additive manufacturing is a new generation of manufacturing technology and recently it has increasing demand in industrial applications. In this production technique, instead of removing the material, the material is added layer by layer in order to get a near or net shape of the full geometry. Thus, the final shape of the products can be produced with use of less material and more complex shape of products can be produced easily. In this work, shaped metal deposition (SMD), which is one of the additive manufacturing methods, was used for producing cylindrical parts. For this purpose, an experimental set-up including TIG welding + wire deposition tool was designed and constructed. The aim of this work is to investigate the cylindrical part manufacturing using SMD method and analyse geometrical attributes, macro and microstructure characteristic as well the effects of as the process parameters. The geometry of the deposited parts was investigated using a suitable design of experiment. The effects of the process parameters on wall height, width, and outer diameter were also investigated. The optimum set of parameters was obtained to produce cylindrical parts as: current (I)=120 A, travel speed (TS)=0.18 m/min and wire feed speed (WFS)=1.9 m/min. Furthermore, the metallographic testing results showed that TS and I values were very effective on microstructure and the changes in the value of WFS had not a significant effect on the microstructure. Vermicular and lathy ferrite morphology were observed on the investigated microstructures because of the cooling effect. For some samples, the content of the vermicular ferrite was found more than the others. The macrostructure results showed that there were no errors in the depositions, even on the interface between successive layers. It has been found that the hardness was affected by the amount of heat input to the deposition area.

Key Words: Shaped metal deposition, additive manufacturing, near-net shaped manufacturing, TIG welding

ÖZET

ŞEKİLLİ METAL YIĞMA YÖNTEMİYLE SİLİNDİRİK PARÇA ÜRETİMİNİN ARAŞTIRILMASI

KESKİN, Ömer Özden

Yüksek Lisans Tezi, Makine Mühendisliği Bölümü

Tez Yöneticisi: Doç. Dr. Oğuzhan YILMAZ

Ağustos 2016

57 sayfa

Katmanlı imalat, yeni nesil imalat teknolojileri arasında yer alan ve endüstriyel uygulama alanı gittikçe artan bir imalat yöntemidir. Bu üretim tekniğinde konvansiyonel üretim tekniklerine kıyasla, malzeme boşaltma yerine katman şeklinde malzeme yığılması prensibine uyularak, parça geometrisi yaklaşık ve/veya tam parça geometrisine uygun olarak eklemeli bir biçimde üretilmektedir. Böylelikle daha uygun malzeme oranlarında son şekle yakın ve karmaşık geometrili parçaların üretimi mümkün olmaktadır. Bu çalışmada katmanlı üretim yöntemlerinden birisi olan şekilli metal yığma metodu silindirik parça üretimi için kullanılmıştır. Bu amaçla TIG kaynak + tel yığma araçları tasarlanmış ve kurulmuştur. Bu çalışmada metal yığma metodu kullanılarak silindirik parça üretme, geometrik özellikleri analiz etme, makro ve mikro yapı analizlerinin yanı sıra işlem parametrelerini de yığılan parçaları analiz etme amaçlanmıştır. Uygun bir deney tasarımı kullanılarak yığılan parçaların geometrisi incelenmiştir. Aynı zamanda, işlem parametrelerinin yükseklik, genişlik ve dış çap üzerindeki etkileri araştırılmıştır. Örnek silindirik parça üretiminde en uygun parametreler akım (I)=120 A, dönme hızı (TS)=0.18 m/d, tel besleme hızı (WFS)=1.9 m/d olarak belirlenmiştir. Ayrıca, metalografi test sonuçları TS ve I parametrelerinin mikro yapıyı etkilediğini, WFS değerlerinin ise mikro yapıyı değiştirmediklerini göstermiştir. Mikro yapı araştırmaları sırasında vermicular ve lathy ferrit morfolojisi soğumanın etkisinden dolayı gözlemlenmiştir. Bazı örnekler için vermicular ferrite yapısı diğerlerinden daha çok görülmüştür. Makro yapı sonuçlarına göre ardışık katmanlar arasında herhangi bir hata gözlemlenmemiştir. Yığma bölgesine giren ısı, sertlik değerini etkilemektedir.

Anahtar Kelimeler: Şekilli metal yığma, katmanlı üretim, nete yakın şekilli parça üretimi, TIG kaynağı



For my family...

ACKNOWLEDGMENTS

The hesitate to share all the information with me during this work, with great effort in my thesis, at the same time as me so much personality Assoc. Prof. Dr. Oğuzhan YILMAZ, I would like to say special thanks for everthing, his support for time off to work to research and write my dissertation was truly helpful and greatly appreciated.

I would like to acknowledge to my friend Adnan A. UGLA for his valuable friendly help in analyzing and thesis writing process.

Further acknowledgement and thanks to Gaziantep University Department of Mechanical Engineering due to providing financial support in this study.

A very special thanks is due to my parents for their faith in me and for everything that helped me get to this day.

I would like to thanks to Gaziantep University Department of Mechanical Engineering Labratory workshop staff Mehmet TAŞDEMİR, Mehmet YILDIZ and Seyit BOSTANCIERİ.

Finally, thanks for love, patience and support from my friend İpek NACAR. I could not have completed my research without the support of all these wonderful people.

TABLE OF CONTENTS

	Page
ABSTRACT.....	v
ÖZET	vi
ACKNOWLEDGMENTS	viii
TABLE OF CONTENTS	ix
LIST OF TABLES	xi
LIST OF FIGURES	xii
LIST OF ABBREVIATIONS	xiv
LIST OF SYMBOLS	xv
1. INTRODUCTION	1
1.1. Introduction	1
1.2. Scope of Thesis	2
1.3. Aim of Thesis	2
1.4. Outline of the Thesis	2
2. LITERATURE REVIEW.....	3
2.1. Introduction	3
2.2. Additive Manufacturing	3
2.3. Shaped Metal Deposition	4
2.4. Circular Metal Deposition (CMD) Machine Unit	6
2.5. Microstructure Austenitic Stainless Steel	6
3. EXPERIMENTAL SETUP AND MATERIAL.....	10
3.1. Introduction	10
3.2. Experimental Setup Design and Construction	10
3.2.1. Calculation of Travel Speed	21
3.3. Circular Metal Deposition Machine Units	14
3.4. Material	15

3.5. Design of Experiment.....	16
3.5.1 Geometrical Measurement.....	18
3.5.2. Metallographic Testing.....	19
3.5.2.1. Sample Preparation.....	19
3.5.3. Hardness Test	21
4. RESULTS AND DISCUSSION	22
4.1. Introduction	22
4.2. Geometrical Analysis	22
4.2.1. Control of The Bead Height	23
4.2.2. Control of The Outer Diameter	24
4.2.3. Control of The Bead Width	25
4.3. Macrostructural Analysis	27
4.4. Microstructural Analysis	29
4.4.1. Effect of Travel Speed on Microstructure	30
4.4.2. Effect of Current on Microstructure	31
4.4.3. Effect of Wire Feed Speed on Microstructure.....	32
4.5. Weld Defects	33
4.6. Hardness	33
5. CONCLUSIONS.....	35
5.1. Future Work	37
REFERENCES.....	38
APPENDIX.....	42
APPENDIX A: Welding Machine Technical Specifications.....	42

LIST OF TABLES

	Page
Table 2.1. Austenite stainless steel solidification types	7
Table 3.1. CMD machine part list	11
Table 3.2. CMD machine reducer specification	13
Table 3.3. The chemical composition of the substrates and the filler materials	16
Table 3.4. Nominal pre-set operating conditions	17
Table 3.5. The main process parameters and their levels	17
Table 3.6. The experiment layout and process parameters	18
Table 4.1. The experiments geometrical dimensions results and picture	23
Table A.1. TIG welding machine technical specification	43

LIST OF FIGURES

	Page
Figure 2.1. Pseudobinary section of the Fe-Cr-Ni ternary system at 70% Fe	8
Figure 2.2. Relationship of solidification type to the Pseudobinary phase diagram	8
Figure 3.1. Schematic view of CMD machine CAD design	11
Figure 3.2. (a) Schematic diagram of the experimental set-up, (b) picture of the deposition process	12
Figure 3.3. Screw and nut	13
Figure 3.4. Circular Metal Deposition machine unit	15
Figure 3.5. Geometrical measurement point for h,w and D_o	19
Figure 3.6. (a) Cutting schedule, (b) after cutting	19
Figure 4.1. Schematic representation for deposition part	23
Figure 4.2. Main effects of the process parameters on bead height	24
Figure 4.3. Main effects of the process parameters on the outer diameter	25
Figure 4.4. Main effects of the process parameters on the bead width	26
Figure 4.5. (a) A sample cylindrical geometry made by CMD, (b) a sample of after machining	27
Figure 4.6. Macrograph shows the cross-section of the deposited wall	28
Figure 4.7. Macrostructure and micrograph of experiment number 27	28
Figure 4.8. Micrograph shows the microstructure of top area in experiment number 22.....	30
Figure 4.9. (a) Experiment number 3 (TS = 0.1 m/min) vermicular morphology, (b) experiment number 6 (TS = 0.28 m/min) lathy morphology	31

Figure 4.10. (a) Experiment number 18 ($I = 105 \text{ A}$) lathy morphology, (b) experiment number 27 ($I = 120 \text{ A}$) vermicular morphology 32

Figure 4.11. (a) Example number 26 ($\text{WFS} = 1.9 \text{ m/min}$) and (b) example number 27 ($\text{WFS} = 2.1 \text{ m/min}$) lathy morphology 32

Figure 4.12. Plot illustrate main effect parameters on hardness 34

Figure A.1. TIG welding machine 42



LIST OF ABBREVIATIONS

RP	Rapid Prototyping
RM	Rapid Manufacturing
AM	Additive Manufacturing
ASTM	American Society for Testing and Materials
DLD	Direct Laser Deposition
EBD	Electron Beam Deposition
SMD	Shaped Metal Deposition
3D	Three - Dimensional
TIG	Tungsten Inert Gas
SMDPTW	Shaped Metal Deposition by Pulsed TIG Welding
CMD	Circular Metal Deposition
MIG	Metal Inert Gas
WAAM	Wire + Arc Additive Manufacturing
LM	Laser Melting
UAM	Ultrasonic Additive Manufacturing
PD	Plasma Deposition
GWAM	Gas Metal Arc Welding
RAPOLAC	Rapid Production of Large Aerospace Components
AMRC	Advanced Manufacturing Research Center
CNC	Computer Numerical Control
A	Austenitic
AF	Austenite + Eutectic Ferritic
FA	Ferrite to Austenite
F	Ferrite
CAD	Computer Aided Design

LIST OF SYMBOLS

i	Transmission Ratio
I	Current
Ø	Diameter
α	Feeding Angle
TS	Travel Speed
sec	Second
min	Minute
m	Meter
AC	Alternative Current
DC	Direct Current
l	Liter
WFS	Wire Feed Speed
DOE	Design of Experiment
h	Height
w	Width
D	Center Diameter
N	Revolution
D_o	Outer Diameter
rpm	Revolutions Per Minute
gr	Gram
V	Volt
ml	Milliliter
HR	Hardness Rockwell
mm	Milimeter
A	Amper

CHAPTER 1

INTRODUCTION

1.1.Introduction

Shaped metal deposition is known as a rapid manufacturing (RM) technique that directly uses CAD data in order to produce functional metallic parts which are dense, metallurgical bonded, and relatively having geometric accuracy and surface quality. A weld-based manufacturing is one of the techniques that offer a promising approach to satisfy the requirements of producing near-net shaped parts [1]. In aerospace and other high-level industries, metal parts are mostly produced by machining, casting and forging to obtain a designed shape. An expensive manufacturing process requires huge amount of work, special tooling and causes noticeable waste. Companies are increasingly inclining towards RM for its economic and environmental advantage over other general manufacturing methods. High-level industries are predicted to produce about 20 million tonnes of waste material over the next 20 years [2]. With machining rates and ever increasing material costs especially in titanium, the waste from the usual manufacturing strategies will pile up. In addition, these are more acceptable and demanded for new manufacturing techniques.

Additive Manufacturing (AM) is a different technique to produce complex, near-net shaped metal components in layer by layer manner. In this technique, short lead-times are obtained and design changes can easily be incorporated. It minimizes wide machining, material costs and consumption of material, leading to a lower environmental effect with a good economic balance [3-6]. According to the ASTM (American Society for Testing and Materials) industry standards [7], AM is defined as the process of weld materials to make objects from 3-D model, generally layer by layer, as oppose to subtractive production technologies [8-10]. It is well known that there are many problems in machining of some materials such as titanium, nickel etc. through general manufacturing technique [11, 12].

1.2. Scope of Thesis

Shaped metal deposition (SMD) is an additive manufacturing method, which can be used to produce near-net shaped metal components. Such metal parts are produced by depositing the melted materials on a substrate layer by layer along a defined path. This technique has some benefits (short lead times, less waste materials and overall cost etc.) in comparison with traditional manufacturing processes like casting, forging or machining. Therefore, SMD has been preferred to produce middle size and large structural metal parts having superior mechanical properties and less raw materials.

1.3. Aims and objectives

This research work aims to develop and investigate TIG + wire deposition process to be used for producing near-net shaped cylindrical parts. This work also aims to investigate the geometrical attributes, microstructural and mechanical properties of the deposited cylindrical parts. To do that, an experimental SMD machine composed of a pulsed TIG welding source, a welding torch and a 2-axis table and cold wire feeding mechanism has been developed.

1.4. Overview of the Thesis

This work consists of four chapters and these are:

Chapter 1 gives a brief introduction about research performed.

Chapter 2 is summarising the related area of this thesis.

Chapter 3 explains the design of experimental setup, materials, and analysis procedure. The Circular Metal Deposition (CMD) experimental setup is explained and then the design of experiments and material is presented.

Chapter 4 includes the results of the geometrical analysis and the parameters. The microstructure and macrostructure of the produced parts are explained. Finally, weld defects and hardness tests results are presented.

Chapter 5 concludes the thesis by giving a summary of the whole work and further works.

CHAPTER 2

LITERATURE SURVEY

2.1. Introduction

This chapter includes the related area of this thesis, which is Wire + Arc Additive Manufacturing (WAAM) process. WAAM process uses arc welding techniques and consequently, the process was investigated thoroughly to gain the in-depth idea. In addition, a particular attention is focused on the cylindrical part manufacturing using welding processes and the latest technology techniques are disputed and their advantages and weaknesses are also briefly described.

2.2. Additive Manufacturing

The process of joining or adding materials with the primary aim of making objects from 3D model data using the layer by layer principle is known as AM. Rapid manufacturing (RM) or rapid prototyping (RP) are the layer manufacturing technologies which are well known among both engineering and scientific communities [13-17].

Unlike machining and stamping, additive manufacturing technique creates final shapes by the addition of materials and these are not similar to conventional manufacturing techniques and prone to fabricate products by removing material from a larger stock or sheet metal. This creates effective and efficient use of available raw materials and produces minimal waste. Also, it offers satisfactory accuracy in the finished parts geometry [18-23]. Additive manufacturing permits a design in the form of a computerized 3D model to be easily transformed to a finished end product without the use or aid of any additional fixtures and cutting tools. Additive manufacturing benefits can lead to new innovations in design and it is a necessary process for the manufacturing and assembly of any product [22, 23].

AM techniques are consisting of several groups, such as Laser Melting (LM), Ultrasonic Additive Manufacturing (UAM), Electron Beam Melting (EBM), Plasma Deposition (PD), and Gas Metal Arc Welding (GWAM) etc. Furthermore, it can also be classified according to material feeding methods namely metallic wire and metallic powder. Developing AM techniques depend on the joining together the different heat sources with different material feeding methods [24-26]. The most suitable classification of the AM processes was done by Yilmaz and Uglu [26]. In their study, they discussed and classified the processes according to the melting heat source used. Additionally, they classified the SMD techniques into three groups based on the heat source.

The most popular method in AM is combination of the laser and powder. With the aid of highly focused laser power and correctly controlled powder feeding, the parts can be fabricated with detailed features and with high accuracies. Several results have been published on this subject for powder feeding with laser [13-16]. Robotic system was used by some works where a SMD cell contains a TIG welding torch attached to a 6-axis robot linked to 2-axis table.

2.3. Shaped Metal Deposition

Wire + Arc Additive Manufacture technique can be classified into two or three main processes based on the type of electric arc torch used to melt and fuse the wires;

- Tungsten inert gas arc welding (TIG welding) + wire deposition
- Metal inert gas arc welding (MIG welding) + wire deposition
- Plasma welding + wire deposition

The wire is fed into the melted pool and melting is also produced by the electric arc source. Wire + Arc AM technique has high deposition rate and 100% efficiency and for this reason, it has gained considerable interest in the recent years.

This process is also called as Shaped Metal Deposition technique. In this process, an argon flooded hood with a 2 axis rotating table, wire feeding system and the electric arc torch are used. Apart from that, in some cases, deposition can also be performed in an argon floated chamber and does not require vacuum environment as EBD [18].

Recently, wire was used instead of powder, due to the fact that it facilitates increased deposition rates, decreased contamination problems and reduces the high costs of powders. The continuous wire feed provides high deposition rate and furthermore, less manufacturing time for large aerospace structural components [11].

Many researchers have been studying basic characteristics of wire based additive manufacturing by using TIG welding machine as a melting source during deposition processes for depositing Ti-6Al-4V. They used pulsed TIG welding machine associated with robotic system, see, e.g. [3-6], [9] and [10]. Oguzhan and Uglu [27] investigated the characterization of the macrostructure and microstructure of austenitic stainless steel using pulsed current TIG arc shaped metal deposition. There are no similar works exactly aiming at SMD with pulsed TIG wire feeding process for high-grade stainless steel as additive manufacturing method.

The SMD process was further improved by a European project called Rapid Production of Large Aerospace Components (RAPOLAC) [28], which was initiated in 2005 by the Advanced Manufacturing Research Centre (AMRC) at the University of Sheffield in collaboration with seven partners from across Europe. The objective of this project was to build large parts with a variety of aerospace materials [3-5], [9], [10], [24], [25] and [29]. Skiba and Baufeld [29] produced round parts by using 308 materials.

Broadly, some of the researchers were aimed at comparing different methods (i.e. Laser, Arc), see e.g. [24-26]. Compared to the AM processes by using laser plus powder or wire solutions, the system for the WAAM process is much cheaper and easier to build. The power efficiency and productivity of the WAAM process is much higher than the laser based system. These inherent process advantages make the WAAM process especially suitable to be used for fabricating large scale components. However, due to the process constraints of arc welding, the complexity of the WAAM components is comparatively low. The finishing quality is not as good as the laser-based AM processes.

The arc welding techniques with wire feeding combines wire and arc manufacturing (WAAM) process and standard wire-based welding processes such as Metal Inert Gas (MIG) and Tungsten Inert Gas (TIG) employed as heat sources due to low cost.

As the system can be easily mounted on industrial robots and CNC machines, it is possible to fabricate large scale components.

Nowadays, many of researchers used this technique to fabricate different metallic features components. Yilmaz O. and Uglu A. A. [11] developed a new SMD integrated system to manufacture different geometries of metallic parts. Wang and Kovacevic [1] used SMD to produce cylindrical deposited parts. In this study, different materials were used and the geometries were compared. A few studies investigated the control of different experimental methods; see e.g. [30-32]. Large body of studies on WAAM-SMD were performed using complex robotic systems [3, 4, 9].

In this thesis, AM process is focused on metallic materials only. Different techniques and concepts have been developed in the metal AM area during the recent years to provide industry with light weight and fully functional metallic parts. The Circular Metal Deposition (CMD) machine was designed and fabricated. The developed CMD system is used in the manufacturing of cylindrical parts with different sizes and height. In this method, there is no computer control unit. Therefore, the system is simple and convenient. Complex programming languages were not used.

2.4. Circular Metal Deposition (CMD) Machine Unit

CMD machine unit is a specifically designed system to manufacture cylindrical geometry parts. TIG welding machine consists of wire feeding unit and CMD machine. CMD machine unit provides the cylindrical deposition by using SMD method. Simultaneously, rotational table is capable of rotational and axial movement. Rotation speed can be adjusted and with axial movement, up or down progress is stabilized. All system movement is provided by means of a single motor and reducer. The system is simple, stable and useful. 2-D parts can be produced without computer control unit.

2.5. Microstructure Austenitic Stainless Steel

Microstructural analysis of austenitic stainless steel is extremely important in today's world where metals, ceramics, polymers, and composites are used to improve our everyday lives by ensuring safety and reliability in the products that we use. In order, to correctly analyse these microstructures, proper specimen preparation is required to

eliminate preparation induced microstructural artefacts. In general, minimizing the damage early in the microstructural preparation stage by choosing the correct abrasive, lubricant, and equipment parameters, the steps required to highlight the representative materials microstructure can be obtained by following the basic steps.

Austenitic stainless steels represent the largest of the general groups of stainless steels and are produced in higher tonnages than any other group. Austenitic stainless steels are widely used in several industries because of their excellent corrosion resistance as well as their good mechanical properties [33, 34]. General austenitic stainless steel welding consumables such as type 308 and 308-L are designed so that the weld metals contain approximately 3-10% ferrite in order to prevent hot cracking and minimize the high-temperature embrittlement [35].

There are four solidification and solid-state transformation possibilities for austenitic stainless steel weld metals. These reactions are listed in Table 2.1 and related to the Fe-Cr-Ni phase diagram in Figure 2.1 [36]. Note that A (austenitic) and AF (austenite + eutectic ferritic) solidification modes are associated with primary austenite solidification, whereby austenite is the first phase to form upon solidification. Following solidification, additional microstructural modification occurs in the solid state for the FA (ferrite to austenite) and F (ferrite) types, due to the instability of the ferrite at lower temperatures as shown in Figure 2.2. The various microstructures that are possible in austenitic stainless steel weld metals are presented [36].

Table 2.1. Austenite stainless steel solidification types

Solidification Reaction and Resultant Microstructure		
Solidification Type	Reaction	Microstructure
A	$L \rightarrow L+A \rightarrow A$	Fully austenitic, well-defined solidification structure
AF	$L \rightarrow L+A \rightarrow L+A+(A+F)_{eut} \rightarrow A+F_{eut}$	Ferrite at cell and dendrite boundaries
FA	$L \rightarrow L+F \rightarrow L+F+(F+A)_{per/eut} \rightarrow F+A$	Skeletal or lathy ferrite resulting from ferrite-to-austenite transformation
F	$L \rightarrow L+F \rightarrow F \rightarrow F+A$	Acicular ferrite or ferrite matrix with grain boundary austenite and Widmanstätten side plates

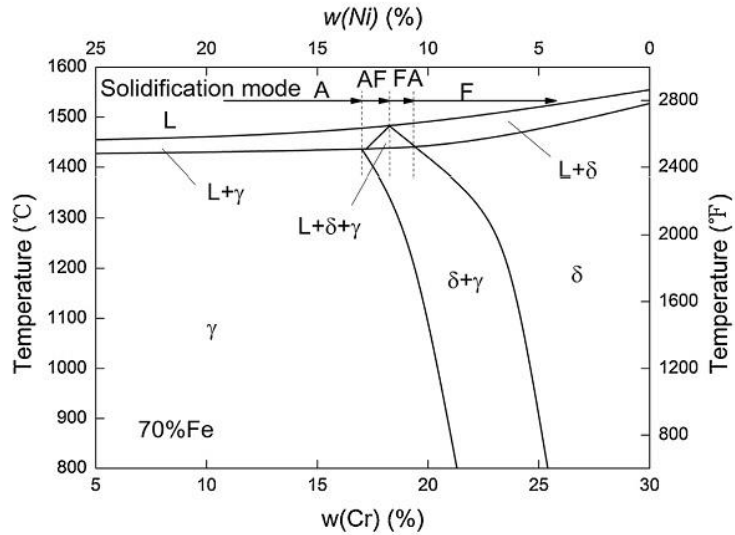


Figure 2.1. Pseudobinary section of the Fe-Cr-Ni ternary system at 70% Fe [37]

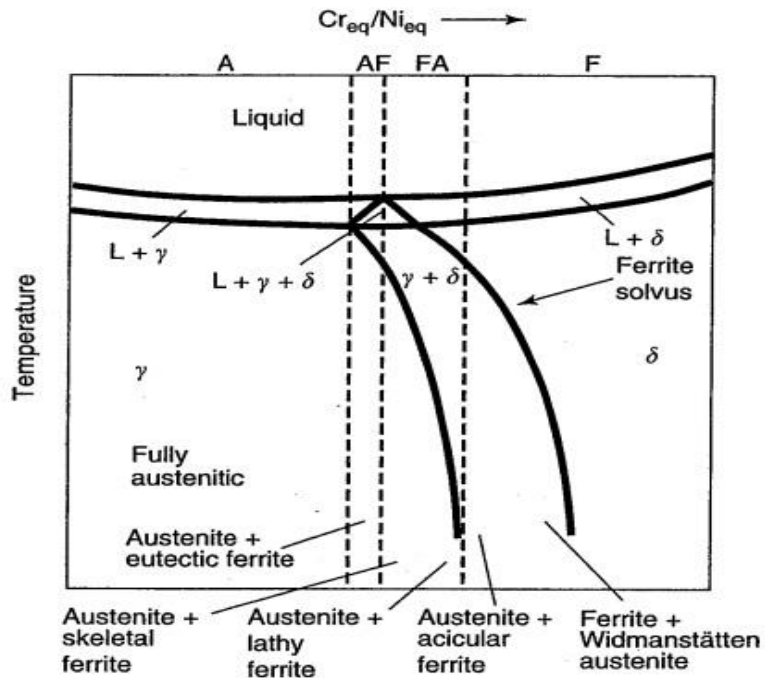


Figure 2.2. Relationship of solidification type to the Pseudobinary phase diagram [36, 38]

Full austenite solidification (A): The metal entirely solidifies as austenite and remains in this phase to room temperature and exhibits a distinct solidification structure when viewed metallographically [36,38].

Primary austenite solidification (AF): If some ferrite forms at the end of primary austenite solidification process via a eutectic reaction, solidification is termed Type AF. If the material cools down under equilibrium conditions, the ferrite will

transform to austenite, but under rapid cooling ferrite will remain to room temperature [36,38].

Primary ferrite solidification (FA): When solidification occurs as primary ferrite and at the end of solidification some of the austenite forms, it is termed Type FA. When cooling down the metal under equilibrium condition, the ferrite can be transformed to austenite. However, under rapid cooling rate, some of the ferrites will remain to room temperature [36,38].

Ferrite solidification (F): If solidification occurs completely as ferrite, it is termed Type F. In this case the microstructure is fully ferritic at the end of solidification. When cooling down, it may transform partially or totally to austenite [36,38]. Stainless steels that solidify in the primary ferrite FA are the most resistant to hot cracking.

CHAPTER 3

EXPERIMENTAL SET-UP AND MATERIALS

3.1. Introduction

This chapter gives the details of the designed and constructed Circular Metal Deposition machine, the test apparatus and materials used. In addition, the design of the experiment and the test plan are explained. Finally, the initial steps for operations analysis after the test are explained in detail.

3.2. Experimental Set-up Designing and Construction

In order to conduct the SMD process experimentations, a two-axis machine was designed and constructed. First of all, the design was accomplished by using CAD software according to the valid standards. A deposition unit was used to attach the welding torch and wire feed nozzle. The designed machine is integrated with a machine body, a fixed arm which is used for holding the deposition tool at constant position (X and Y axis), and a rotating table (Z-axis). The rotating table moves only in Z-direction with high flexibility concerning the size and shape of the component to be produced with smooth motion at this direction, and adjustable fixtures which are used for holding torches of deposition tool. Figure 3.1 shows the general view the CMD machine unit. The wire is fed into the deposition zone through a circular feed pipe and it is controlled by a wire feed unit. The wire diameter is suitable to be $\text{Ø}0.8$ mm since it is convenient for power supply available in this study. The developed experimental CMD system is schematically shown in Figure 3.2. The name of all machine parts and numbers are listed in Table 3.1. It presents one vertical axis and the welding torch by attaching to the Z axis. The Z axis with a fixed speed moves up in order to provide smoother surface [1]. In addition, substrate rotating speed and the height of deposition layer affect moving speed of Z axis.

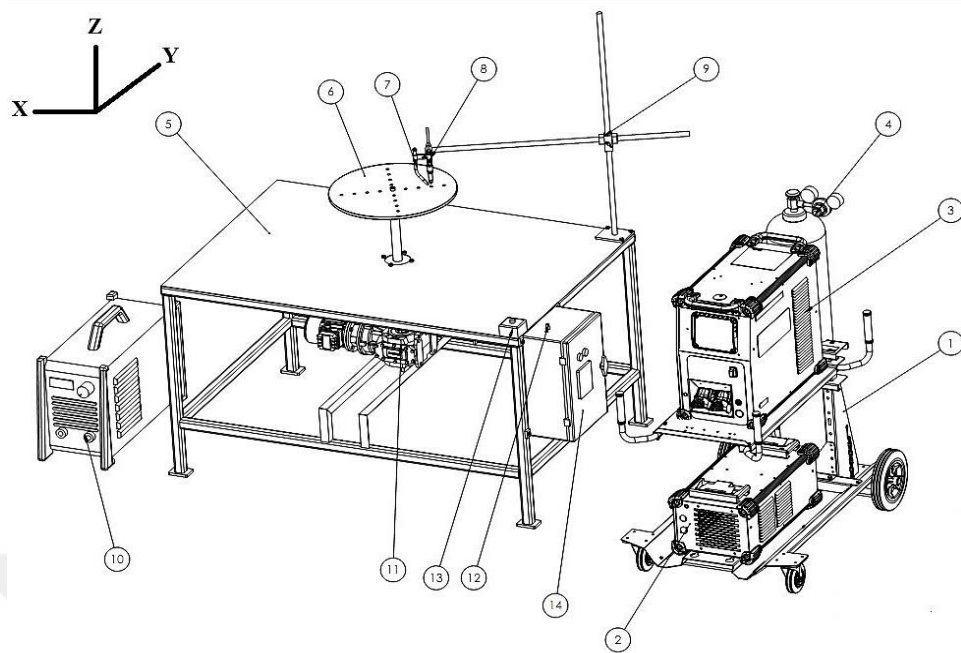


Figure 3.1. Schematic view of the CMD machine CAD design

Table 3.1. CMD machine part list

CMD Machine Parts	
No	Parts
1	Welding machine transport frame
2	Welding machine cooling unit
3	TIG welding machine
4	Argon gas tube
5	Experiment table frame
6	Rotating table
7	Wire feeding torch
8	TIG welding torch
9	Torch holder support arm
10	Wire feeding machine unit
11	Reducer and motor
12	Velocity control button
13	Wire feeding control button
14	Velocity control unit

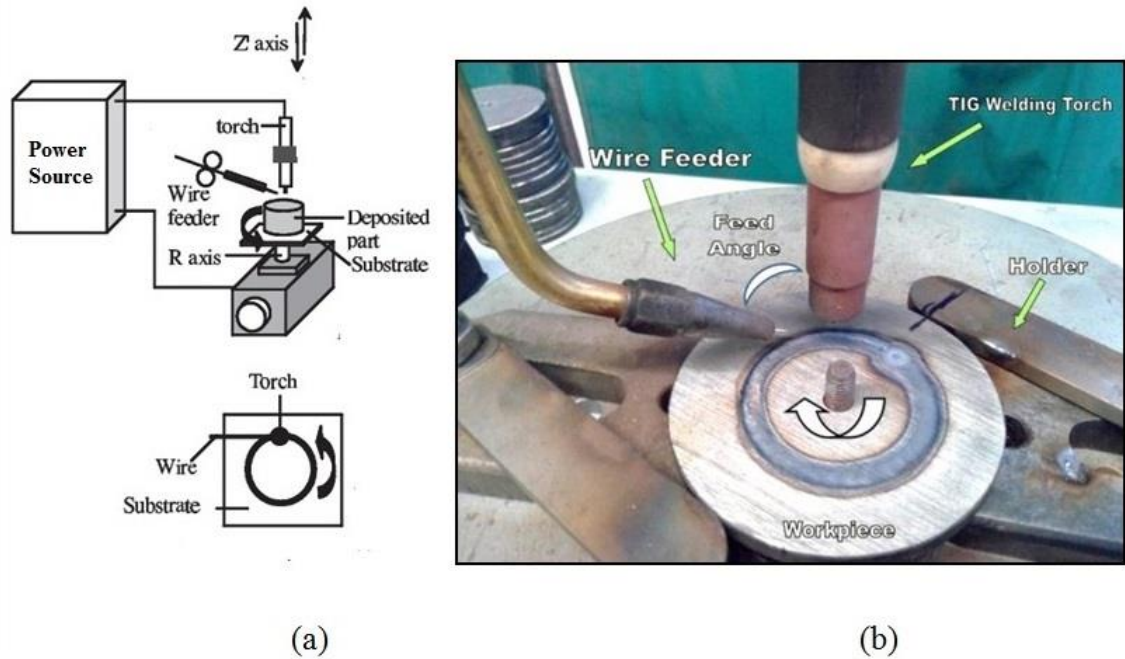


Figure 3.2. (a) Schematic diagram of the experimental set-up, (b) picture of the deposition process

3.2.1. Calculation of Travel Speed

During the experimental setup design, necessary calculations were made for certain parameters. First, the Z-axis linear motion which is associated with the rotational motion of the table was calculated. The rotational speed of table is crucial since it is used as an input to calculate the required travel speed of the system. Accordingly, after the selection of the appropriate motor and speed reduction unit, the manufacturing process is ready to be commenced. Control unit was used to make the experiments with different rotational speeds. In this way, the desired rotational speed is adjusted by reducing the frequency.

In the conducted experimental SMD processes the deposited parts are having 50 mm centre diameter and 20 layers. During TIG welding experiments $\text{Ø}0.8$ mm wire was used and then deposition height was measured in terms of millimetre. After that, travelling rotational table of Z-axis for one tour was decided and for this decision, DIN 13-5 standard fine thread screw shaft, nut, and reduction were selected [39]. In Table 3.2 the properties of used pieces are given. A reduction set was selected according to the designed weight constraints and movement accuracies. The electric motor was selected as having 50 Hz and 0.09 kW power. The reduction transmission

ratio was 175, and the output resolution was calculated as 5.14 rpm. The CMD machine maximum working area was designed as 300 mm in diameter 250 mm in height.

Table 3.2. CMD machine reducer specification

DC Motor	0.09 kW - 50 Hz	900 rpm
Reducer	Ratio = 175	5.14 rpm
Screw shaft and nut	Pitch = 1 mm	d = 28 mm

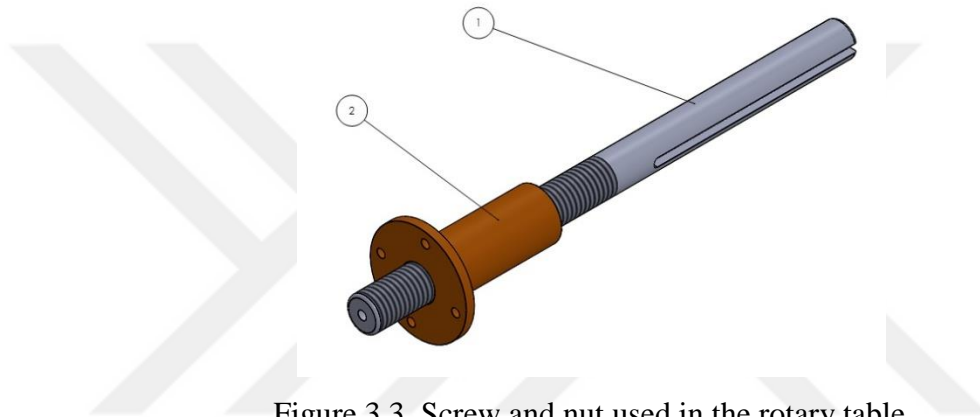


Figure 3.3. Screw and nut used in the rotary table

About 1 mm pitch of the screw and nut were made by using the lathe machine for each turn of rotational table to move 1 mm in Z-axis. As shown in Figure 3.3 the screw shaft (1) and fixed flange nut (2) was designed [40]. Axial and rotational movement is provided by single electrical motor. Deposition process was performed by keeping welding torch arc length.

$$L = p \times n \quad (3.1)$$

Where L refers to lead, p refers to pitch and n refers to number of turns. How many seconds will it take for the deposition process in one tour? This is taken as a reference to determine 3 different rotation speeds in the experimental works. 40, 70, 110 seconds were then determined and according to these values, revolutions per minutes were calculated by using inverter frequency (Hz) values. After that N_1 , N_2 , N_3 were calculated respectively as 0.66, 1.16 and 1.83.

The revolution values were calculated to be required for three different rotational speeds. Accordingly, the experimental study was performed by setting the desired set value from the inverter. The rotational speeds were calculated as follows;

$$TS = \frac{\pi \times D \times N}{1000} m/min \quad (3.2)$$

Where;

D = Center diameter

TS = Travel speed

N = Number of revolution

$$TS_1 = \frac{\pi \times 50 \times 0.66}{1000} = 0.1 m/min \quad (3.3)$$

$$TS_2 = \frac{\pi \times 50 \times 1.16}{1000} = 0.18 m/min \quad (3.4)$$

$$TS_3 = \frac{\pi \times 50 \times 1.83}{1000} = 0.28 m/min \quad (3.5)$$

3.3. Circular Metal Deposition Machine Units

The experimental set-up is a modified version of a TIG welding machine including external wire feeding unit (see Figure 3.4). It consists of the following components:

- Water cooled LINCOLN Invertech V320-T AC/DC welding machine
- A 2-axis movable work table and control unit
- Promig (4T) wire feed machine
- Deposition material (Stainless Steel 308)
- LincTorch (LT18W) water cooled TIG torch
- A wire feeder nozzle (see Figure 3.2.b)

The melting source was conducted using water cooled LINCOLN Invertech V320-T AC/DC welding machine (see Appendix A). It can supply welding current with the range of 5-320 A. The TIG torch is LincTorch (LT18W) water cooled duty cycle, 100%, 1.8 cm cup size with 2% throated tungsten. The tungsten electrode distance from the tipping point till the ceramic cup is recommended to be between 4-9 mm. An arc of plasma is formed between the electrode and the substrate.

The deposited material is supplied by a cold wire which is fed into the melting zone through an annular feed nozzle connected to Promig (4T) wire feed machine see Figure 3.4. It independently provides the cold wire to the deposition tool, it can be manipulated manually.

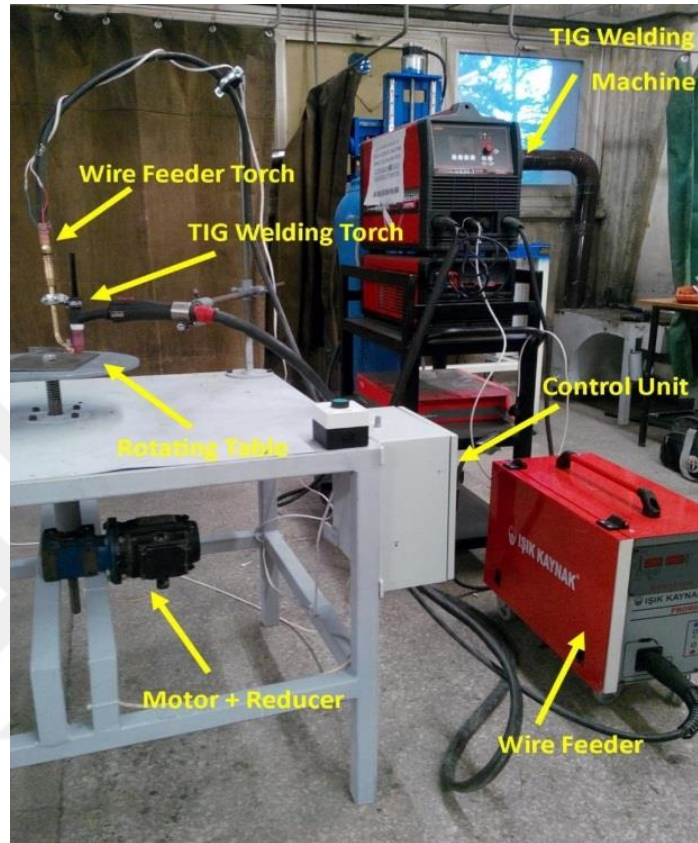


Figure 3.4. Circular Metal Deposition Machine Units

3.4. Materials

The experiments were conducted on as hot rolled low carbon steel type “St. 3” according to DIN standard substrates. The substrates are cylindrical in shape with 8 mm thickness and 100 mm diameters were used as substrates during the experiments. \varnothing 0.8 mm austenitic stainless steel Type 308 LSi solid wire was used as a filler material according to ASTM standard plates [7]. Table 3.3 shows the chemical composition of the substrates and the filler materials. Before the deposition process, these plates were ground to clean the top surface from oxides, grease, paint, rust, etc. To prevent the distortions during high temperature depositions the plates were clamped which also facilitated the heat diffusion [29]. Shielding gas as Argon with a

99.90% was used to prevent gas metal reactions and contaminations. The pre-arranged process parameters used throughout this work are given in Table 3.4.

The grade used in this work is AISI 308 LSi. It has low carbon content to increase the resistance to corrosion, avoid the intergranular corrosion due to sensitization and maintain the mechanical properties. It is very easy to strike and re-strike, so that very smooth, low spatter arc producing a finally rippled bead surface with excellent slag detachability.

Table 3.3. The chemical composition of the substrates and the filler materials

Element	%C	%Si	%Mn	%S	%P	%Mo	%Ni	%Cr	%Fe	Others
Plate Actual (St. 3) Composition	0.067	0.025	0.249	0.01	0.012	0.006	0.015	0.01	Rem
Plate Nominal Composition	0.1 max	0.03- 0.15	0.2- 0.45	0.04	0.04	Rem.
308 LSi as deposition Composition	0.018	0.56	1.358	0.033	0.033	0.115	9.412	19.55	Rem.	Co=0.941 Cu=0.181 Ti=0.057
308 LSi typical Composition	0.012	0.85	1,90	0.002	0.02	0.005	10,50	19,5	Rem.

3.5. Design of Experiment

The SMD system has the capabilities to fabricate fully dense components using solid wire material in a layer by layer manner. Prior to the deposition, it is necessary to carefully tune the main process parameters and conditions such as arc current (I), travel speed (TS), and wire feed speed (WFS). It is essential to know that these factors have to be chosen as suitable as a combination to reach process stability. There are other important conditions which also affect the deposition quality such as shielding gas flow rate, the wire feeding angle (α), wire feed direction and position of the wire tip in the weld pool. These parameters control the amount of heat input, metal deposition rate and the beads geometry.

Several experiments were done in order for tuning the main parameters and conditions. These preliminary experiments were done using filler wire 308 LSi in

order to know the main parameter and other conditions limits and their effects on the bead geometry. The method of experiment was selecting a combination of arc current (I), travel speed (TS), deposit beads with different wire feed speed (WFS) starting from 1.0 m/min and increasing it by 0.3 m/min until the deposition process shows an excess of wire. Then the procedure was repeated from the other sets of arc current and travel speed. The most appropriate parameters were determined using this method according to initial performed experiments.

The process was implemented using Design of Experiment (DOE) methodology by a full factorial method. 3^k factorial design is described as full factorial design. Because by using this method and determined parameters, correct results are obtained in the repeatability experiments. For every three levels, k factors are contemplated. Each 3 levels are expressed as low, intermediate and high. Aim of three-level designs are to figure out the possible skew in the response function and to treat the case of nominal factors at each their levels [41].

The values of the welding parameters and their levels are listed in Table 3.5. The experiments were conducted using the process parameter combination shown in Table 3.6 in order to produce small cylindrical components with bead centre diameter of 50 mm and 20 layers.

Table 3.4. Nominal pre-set process parameters

Shielding Gas	Welding grade Argon
Flow rate	12 l/min
Pre-flow duration	3 sec
Post flow duration	15 sec
Electrode	3.2 mm diameter
Arc length	5 mm
Feeding angle (α)	42°
Wire Stickout	15-20mm

Table 3.5. The main process parameters and their levels

Parameter	Levels		
	1	2	3
Current (A)	90	105	120
Travel Speed (m/min)	0.1	0.18	0.28
Wire Feed Speed (m/min)	1.6	1.9	2.1

Table 3.6. The experiment layout and process parameters

Exp No:	Process parameters			Exp No:	Process parameters			Exp No:	Process parameters		
	Current	Travel Speed	W.F. Speed		Current	Travel Speed	W.F. Speed		Current	Travel Speed	W.F. Speed
1	90	0.1	1.6	10	105	0.1	1.6	19	120	0.1	1.6
2	90	0.1	1.9	11	105	0.1	1.9	20	120	0.1	1.9
3	90	0.1	2.1	12	105	0.1	2.1	21	120	0.1	2.1
4	90	0.18	1.6	13	105	0.18	1.6	22	120	0.18	1.6
5	90	0.18	1.9	14	105	0.18	1.9	23	120	0.18	1.9
6	90	0.18	2.1	15	105	0.18	2.1	24	120	0.18	2.1
7	90	0.28	1.6	16	105	0.28	1.6	25	120	0.28	1.6
8	90	0.28	1.9	17	105	0.28	1.9	26	120	0.28	1.9
9	90	0.28	2.1	18	105	0.28	2.1	27	120	0.28	2.1

3.5.1. Geometrical Measurements

Twenty-seven different parameters are defined by Full Factorial Method. Centre diameter of manufactured parts is 50 mm and they are composed of 20 layers. The geometric measurements are height (h), outside diameter (D_o) and wall width (w). The measurement results are summarized in the next chapter. Different measurements are performed to calculate approximate values and the outer diameter measurement is taken from three different heights as shown in Figure 3.5. The results are listed according to average. In the same way, height and thickness were measured from four different locations by taking their average value.

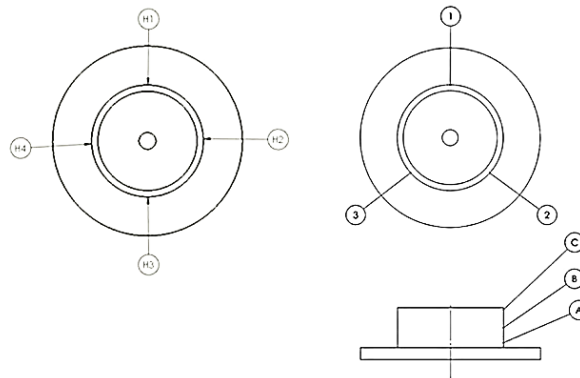


Figure 3.5. Geometrical measurement points for h , w , and D_o .

3.5.2. Metallographic Testing

3.5.2.1. Sample Preparation

A great deal is being written and said about sewing method and probably it is the oldest method in the metallographic laboratory. Besides that, this method is used nowadays in power and band hacksawing [42]. Due to the base plate size used in the experiment, it was necessary to use band hacksawing. Samples were divided into four parts by considering the analysis and tests to be made in the next process. Cutting process is shown in Figure 3.6.

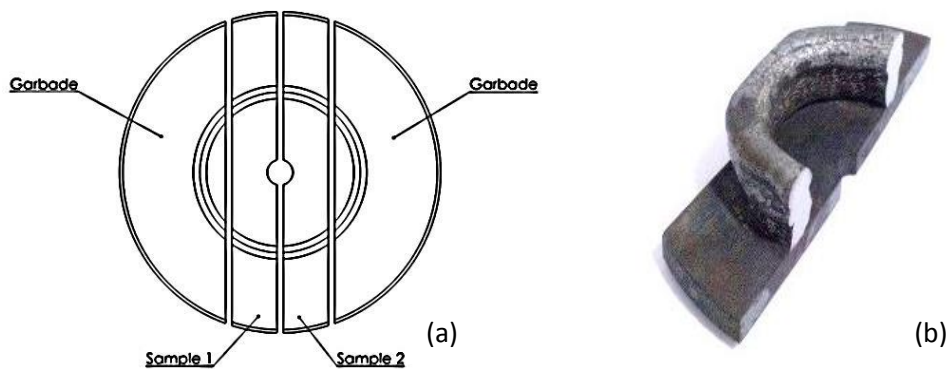


Figure 3.6. (a) Cutting schedule, (b) microstructure specimen

During the sample preparation, grinding operation was important because it provides us with the opportunity to minimize mechanical surface damage by eliminating the need of next polishing process. In addition, mechanical harm can be prevented by extending grinding operation [42]. In the preceding operation, one or two grit smaller

size abrasive should be preferred. Grinding order may include grit sizes of 120, 200, 400 and 600 mesh. In the experiments, respectively SiC abrasive paper is used with hand grinders. After that, samples are ready to be polished by attaching 1000 mesh papers to automatic grinding disk.

Polishing is a technique which is used as a last step to produce scrape free, flat and shiny surface. This technique is important for next accurate metallographic explication namely, qualitative and quantitative. However, in this method, there should not be extrinsic structures like pitting, staining, disturbed metal [42]. The most commonly used polishing abrasive is Aluminium Oxide (alumina). This type of abrasive is useful in terms of polishing. In addition, Al_2O_3 is used as 0.15-0.3 μ [43].

In the experiments, the polishing process was performed by using 1 μ alumina. Rotational speed of the disc was 450 rpm. After polishing, the samples were cleaned with ethyl alcohol. Twenty-seven samples were prepared for etching operation. Etching method is generally used to produce image constant due to improved microstructural features. Broadly, this method can be categorized as optical, electrochemical (chemical), or physical according to the level of process change [43]. With the help of etching, microstructural features like grain size, phase features etc.enhance by changing according to composition, crystal structure, and stress.

In the conventional chemical etching, the etchant reacts with the specimen surface without the use of an external current supply. Etching proceeds by selective dissolution according to the electrochemical characteristic of the component areas. After different etching methods, it was decided that the quickest and very effective method was electrolytic etching. 10 gr Oxalic Acid (CrO_3) + 100 ml distilled water etchant should be used for austenite stainless steel material.

The optical microscope is used to magnify small sample image and are generally known as light microscope. There is lenses system and with the aid of visible light, it is possible to magnify images [44]. Digital microscope uses charge-couple device camera to observe a sample. This microscope enables us to see results on computer screen without eyepieces.

3.5.3. Hardness Test

Objectives of using the hardness test is to monitor the quality control, select process for materials, provide information about tensile strength, wear resistance, ductility and other physical characteristics. In this work, Rockwell Hardness scale A test was used to measure the hardness of samples by using the device “BMS DIGIROCK-RBOV”. The Rockwell Hardness (HRA) scale uses diamond cone indenter forced on sample surface and the hardness value is calculated based on the dent dimension. [45]. Every reading is an average of three-point test where the indents were spaced to equal sides triangle in the center of the specimen. In order to ensure the reliability, after a certain number of tests a standard test block was tested. Hardness test was conducted to show the effects of deposition parameters on the hardness.

CHAPTER 4

RESULTS AND DISCUSSIONS

4.1. Introduction

This chapter discusses the results of the experiments such as macrostructural and microstructural analysis, weld defects and hardness test results. The experiments were analysed using DOE, by using full factorial design method with ANOVA results. Most suitable parameters are determined based on the analysis of the results.

4.2. Geometrical Analysis

The experimental results are shown in Table 4.1. It also demonstrates the capabilities of the developed CMD machine system. A well planned set of deposition parameters were used in experimental SMD trials. Centre diameter of manufactured parts is 50 mm and they are composed of 20 layers. The geometric measurements are height (h), outside diameter (D_o) and wall width (w). The schematic representation of the deposited surface is shown in Figure 4.1.

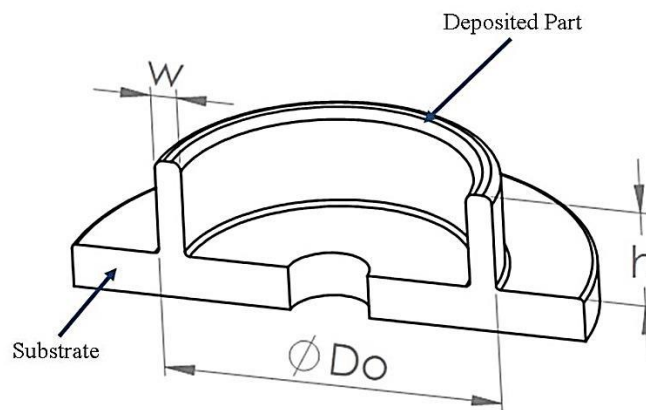


Figure 4.1. Schematic representation of a half-cut deposited part

Table 4.1. Dimensional measurements of the geometrical attributes

Exp No:	Output Responses				Experiments
	Height	Do	Width	Hardness	
1	16,2	51,8	8,5	51,4	
2	22,1	52,7	8,3	50,8	
3	20,3	54,9	7,1	50,6	
4	13,6	52,8	5,8	44,4	
5	9,9	55,7	5,3	45,6	
6	18,8	51,5	5,5	48,4	
7	11,3	51,3	4,8	55,0	
8	14,6	56,2	4,4	54,5	
9	12,5	57,2	5,0	54,6	
Exp No:	Output Responses				Experiments
	Height	Do	Width	Hardness	
10	14,3	52,2	8,0	47,5	
11	13,8	56,7	8,8	52,0	
12	20,3	52,6	8,5	51,8	
13	9,4	54,6	7,4	49,2	
14	11,6	52,6	6,0	50,7	
15	15,8	52,3	6,6	51,1	
16	10,0	55,6	4,9	52,6	
17	10,3	56,2	5,1	52,0	
18	10,7	55,2	4,5	51,1	
Exp No:	Output Responses				Experiments
	Height	Do	Width	Hardness	
19	11,0	54,0	9,1	49,1	
20	13,9	56,7	10,0	51,7	
21	7,8	57,5	9,4	51,5	
22	8,8	56,1	7,0	47,6	
23	10,4	54,6	7,6	50,1	
24	13,8	56,3	7,0	43,9	
25	7,3	52,5	5,2	50,5	
26	9,6	52,7	5,8	51,5	
27	9,5	56,2	5,0	47,6	

4.2.1. Control of The Bead Height (h)

To identify the significant factor effects, an analysis of variance is used. The result of the ANOVA for the main effects of the process parameters on bead height is shown in Figure 4.2. The experimental parts had a range of the wall heights (h) from 7.3 to 22.1 mm. It is clear that the main cause of the total deposition height is the welding current. It is explicit that the most important factor affecting wall height is the I and

TS, whereas WFS has minor effect on height of the part. Decreasing the bead height would implicate increasing the travel speed and current. Besides that, there is a direct relation between the bead height and wire feeding speed. In order to ensure that the SMD process would be uniform, the step height must be kept near to 0.65 mm/layer. As shown in graph when I and TS increase, height decreased. Therefore, the arc length is elongated. Due to elongation of the arc length, the molten metal scattered and height decreased. So the most suitable parameters which make the deposition process more stable would be I=105 A, TS=0.18 m/min, and WFS=1.9 m/min.

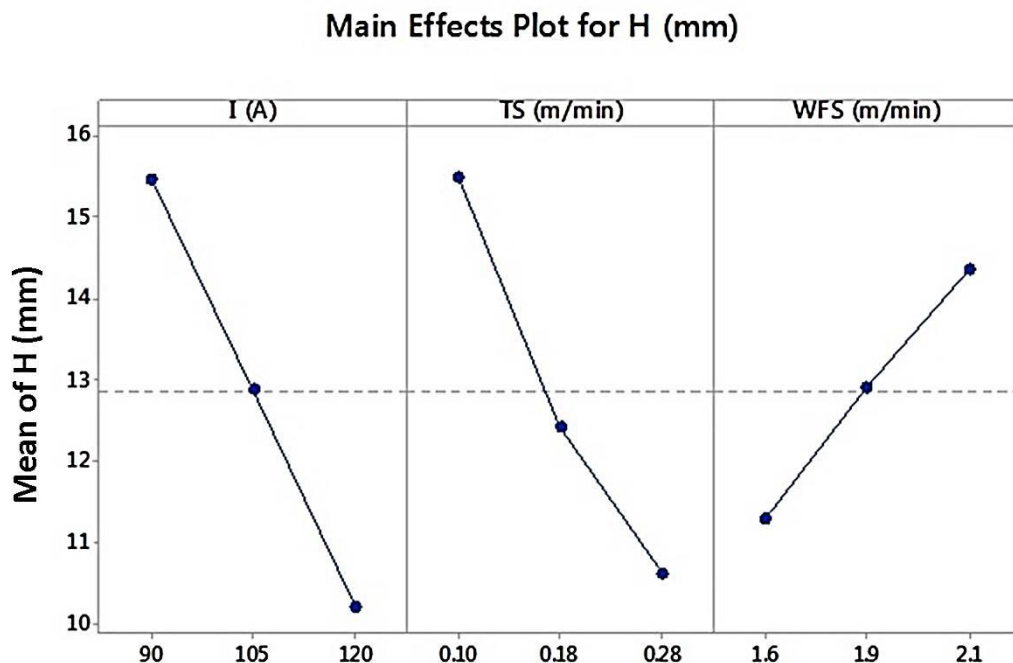


Figure 4.2. Main effects of the process parameters on bead height

4.2.2. Control of The Outer Diameter (D_o)

Using the same method of analysis from the outer diameter. The results of the ANOVA is shown in the Figure 4.3. The manufactured parts in the conducted experiments varied in size with outer diameters ranging from 51.3 to 57.5 mm. Figure 4.3 shows the plot indicating the major factors affecting the values of outer diameter. It can readily be asserted that the most important factors affecting the outer diameter are I and WFS, whereas TS has less effect on height of the part.

Main Effects Plot for Do (mm)

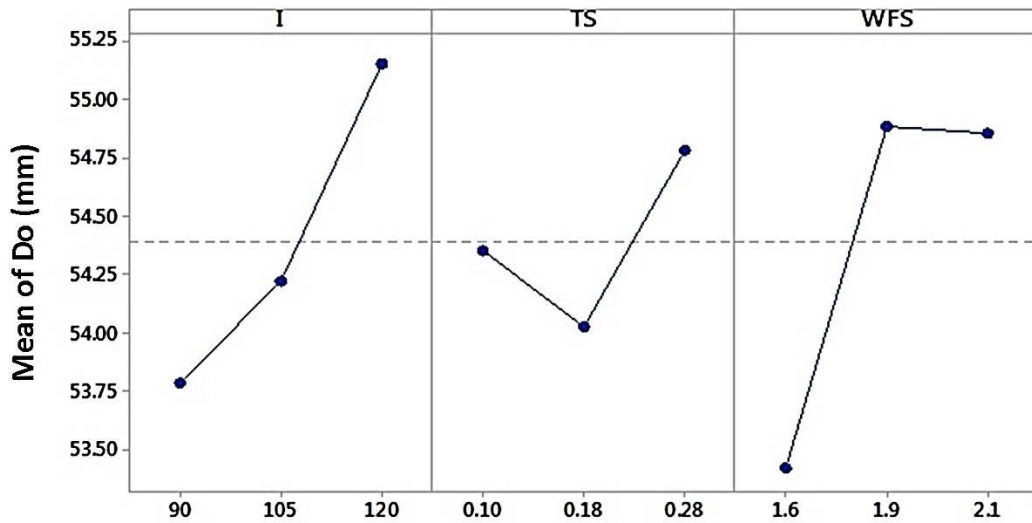


Figure 4.3. Main effects of the process parameters on the outer diameter

Increasing the current also increases the size of the outer diameter, along with the width of the deposit. The outer diameter increases proportional to the feeding speed. When TS increases from 0.1 to 0.18 m/min it can see decreases but when TS increases to 0.28 m/min it can see the D_o increases, this maybe attributed to chance errors such as wrong measurements. According to the desired width of the deposited part, the most suitable parameters which resulted in wall width above 8 mm are (Amperage less than 105 A, TS =0.1 m/min, and WFS =1.9 m/min)

4.2.3. Control of The Bead Width (w)

The results of ANOVA is shown the main parameters affecting the bead width is presented in Figure 4.4. The deposited part widths are within the range varying from 4.4 to 10 mm thickness. There is a direct relation between width of the wall and heat input. Besides that, it also strongly depends on the arc power and travel speed. From Figure 4.4, it is obvious that the width of the wall decreases rapidly with increasing travel speed. The travel speed is inversely proportional to the size of the melting pool and the width of the deposit. Increasing current results in increased heat input to the weld pool and consequently, the bead width thickens. Wire feeding speed affects the width but this effect is not so important in comparison to the other parameters. The

acceptable parameters for the produced parts are ($I=105$ A, $TS=0.18$ m/min, and $WFS = 1.9$ m/min).

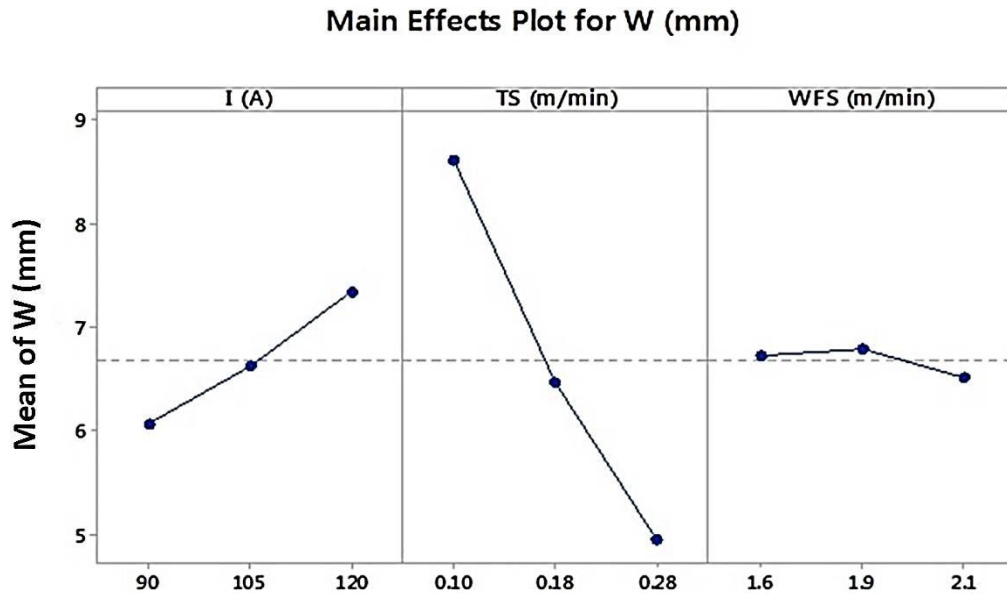


Figure 4.4. Main effects of the process parameters on the bead width

Twenty-seven experimental measurements were carried out and the obtained results are summarised in Table 4.1. According to the results, it can be proved that the most suitable parameters for manufacturing of a cylindrical part for the given material is $I=90-105$ A, $TS=0.1$ m/min and $WFS=2.1$ m/min. For these experiments, these are suitable parameters can be used to manufacture cylinder part. It is obvious that the most suitable height, D_o and w values were obtained in experiment number 3 and 12. Because these part are suitable from the standpoint of geometric desired size. However, it was observed that the deformity at initial layers of experiment number 3 is because of low amperage. Therefore, the experiment number 12 has the most suitable geometric characteristics. Approximately 20-22 mm height, 52-54 mm outer diameter and 8-8.5 mm thickness is obtained in the 20 layer deposition process.

For further applications, the set of parameters used in experiment number 12 can be assigned to obtain acceptable profiles with required dimensions. In order to validate the performance of the developed system, a new experiment was prepared using the most suitable process i.e. experiment number 12 parameters of $I=105$ A, $TS=0.1$ m/min, $WFS=2.1$ m/min to deposit a 32 layers of a center diameter 40 mm cylindrical part with the dimensions shown in Figure 4.5 (a). Total deposition time of

the part was 35 min. Finally, the part was machined using turning machine to the final dimensions shown in Figure 4.5 (b), the total duration of machining was 25-30 min. Figure 4.5 (b) represents a stainless steel type 308 bushing which can be fabricated using CMD machine system with a total manufacturing time about 50-60 min. Consequently, these techniques have process constraints; this means that they may be unable to produce very near shaped components. These methods are not flexible since they are expensive and time-consuming in molds and dies preparation.

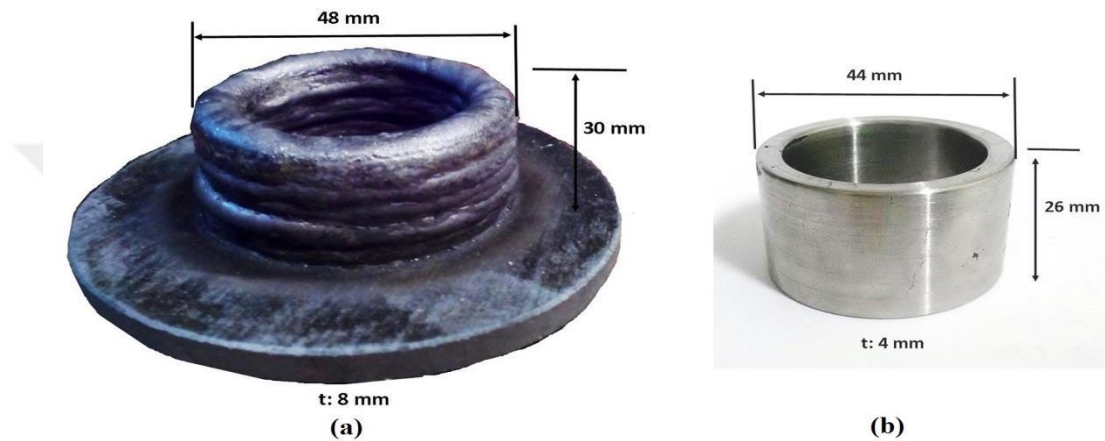


Figure 4.5. A sample cylindrical geometry made by CMD machine (a), a sample after machining (b)

4.3. Macrostructure Analysis

Etched macro-sections showed the traces of the boundaries of the weld metal, fusion boundary, grain growth and the individual runs in multi-layer welds (see Figure 4.6). In addition weld defects such as cracks, porosity, lack of fusion, and lack of penetration can be identified. Macrograph shows the cross-section of the deposited wall in Figure 4.6.

During the deposition process of the specimens, it was observed that in some the layers geometry was disrupted. The macrostructure results show that there are no faults in the interface between successive layers. Figure 4.7 presents the microstructure and macrostructure of the experiment number 27. It can be seen that there is no defect such as porosity and lack of fusions between the layers.



Figure 4.6. Macrograph shows the cross-section of the deposited wall experiment 3 (I=90 A, TS=0.1 m/min, WFS=1.9 m/min)

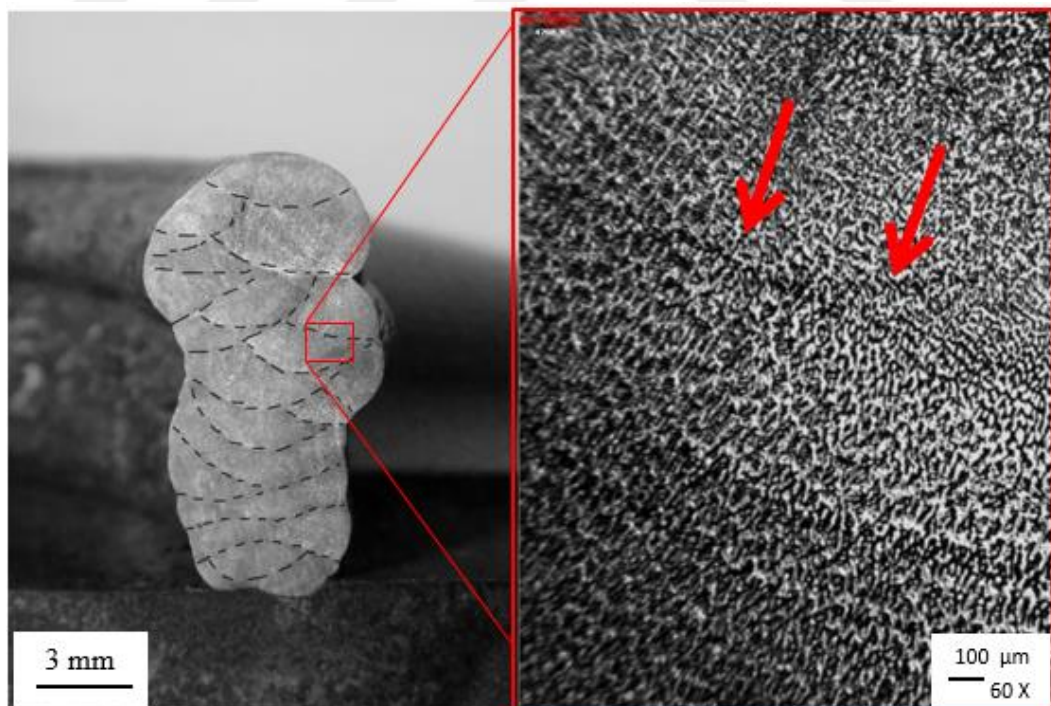


Figure 4.7. Macro and micrograph of experiment number 27 (I=120 A, TS=0.28 m/min, WFS=2.1 m/min)

4.4. Microstructure Analysis

The results of the microstructure analysis indicate that there are four solidification types (A, AF, F, FA) and in this work, the FA type of solidification was observed. Microstructure of FA type solidification is skeletal (vermicular) or lathy ferrite resulting from ferrite to austenite transformation. Formation of some austenite at the end of the solidification means that this is an FA type of solidification. Figure 2.2 shows the relationship of solidification type to the Pseudobinary phase diagram. As can be seen in this figure, these four solidification types are affected by C_{req}/Ni_{eq} ratio and the cooling rates of the samples.

The austenite skeletal (vermicular) ferrite is observed when cooling rate is moderate and the C_{req}/Ni_{eq} ratio is low within FA range. In addition, high cooling rate and increasing ratio of C_{req}/Ni_{eq} would result with austenite lathy ferrite. The place of vermicular morphology creates lathy morphology owing to limited dispersion during austenite ferrite transformation. Transformation is more effective in reducing dispersion distances. This leads to the transformation of more firmly spaced lathy and residual ferrite.

Many sample studies performed have been a cooling medium speed all samples; vermicular and lathy ferrite morphology is observed during the experiments (see Figure 4.8). Content of the vermicular ferrite is more in some samples than the others. Actually, it stems from faster cooling, and micrograph of different microstructures by changing some parameters (I, TS, WFS) are shown below.

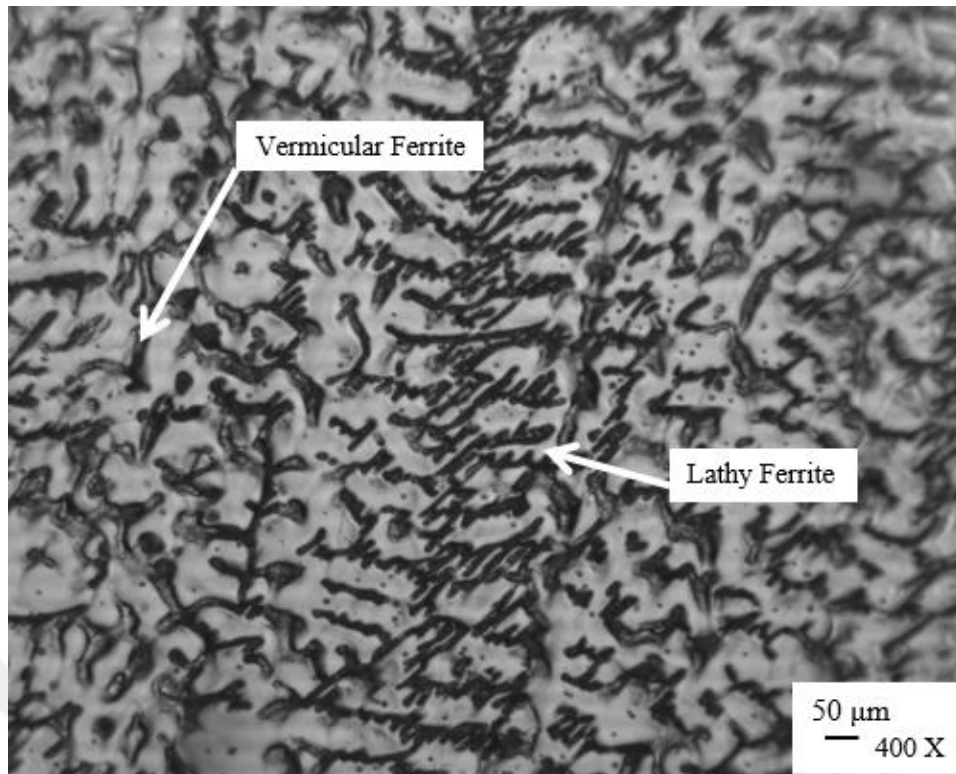


Figure 4.8. Micrograph shows the microstructure of top area in experiment number 22 ($I=120$ A, $TS=0.18$ m/min, $WFS=1.9$ m/min)

4.4.1. Effect of Travel Speed on Microstructure

Figure 4.9 shows the microstructure of the two experiments using the same I and WFS but different TS . The parameters used in both experiments were $I = 90$ A, $WFS = 1.9$. Upper and lower values of TS were compared for two experiments. Fig. 4.9 (a) shows that the grains are relatively larger. This can be attributed to high heat input increase of experiment number 3 ($TS=0.1$ m/min), and so the cooling rate is slower. Vermicular morphology was observed due to low Cr_{eq}/Ni_{eq} ratio. Whereas in experiment number 6, due to TS is high (0.28 m/min), the heat input is less and so the cooling rate is high, which leads to produce fine grains with high amount of residual ferrite as lathy morphology (see Fig. 4.9 (b)).

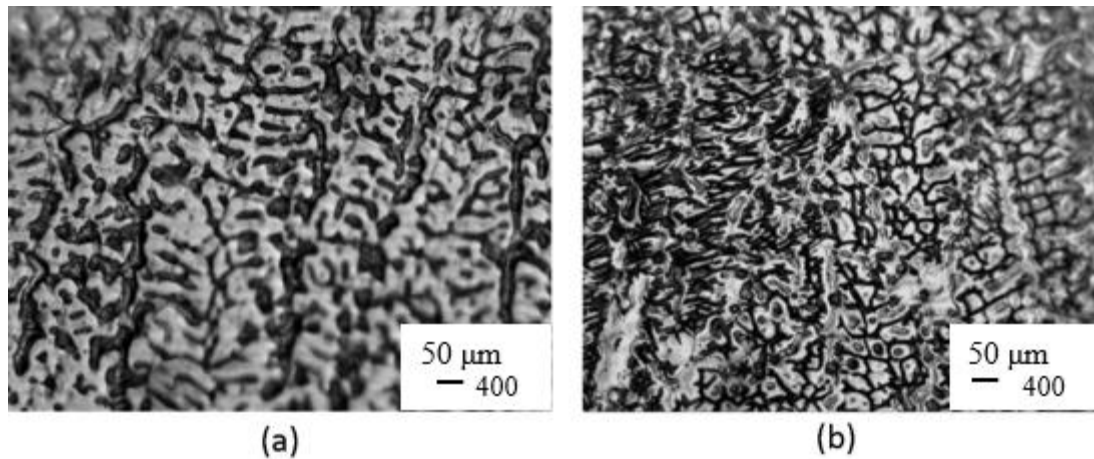


Figure 4.9. (a) Experiment number 3 (TS= 0.1 m/min) vermicular morphology, (b) experiment number 6 (TS = 0.28 m/min) lathy morphology (center point)

Deposition process was completed in a short time due to the high rotational speed. Rapid cooling was observed as temperature of the cylindrical part was not very high. Therefore, lathy morphology was observed.

4.4.2. Effect of Current on Microstructure

Two experiments were performed in order to investigate the effect of welding current on the microstructure of the deposited parts which are the experiments 18 and 27 with currents of 105 A and 120 A respectively. The parameters used in both experiments were TS = 0.28, WFS = 2.1. Figure 4.10 shows the microstructures of the two experiments. In case of I=105 A, the input power is less than that of the second case (I =120 A) and so cooling rate of the experiment 18 is higher than that of experiment 27. This caused a very low Cr_{eq}/Ni_{eq} rate. Therefore, the microstructure of the experiment 18 contains more residual ferrite in lathy form. In experiment number 27, I = 120 A. Material temperature during the deposition process was higher due to the high heat of the arc. This led to the lengthening of the time for cooling. Therefore, vermicular morphology was observed.

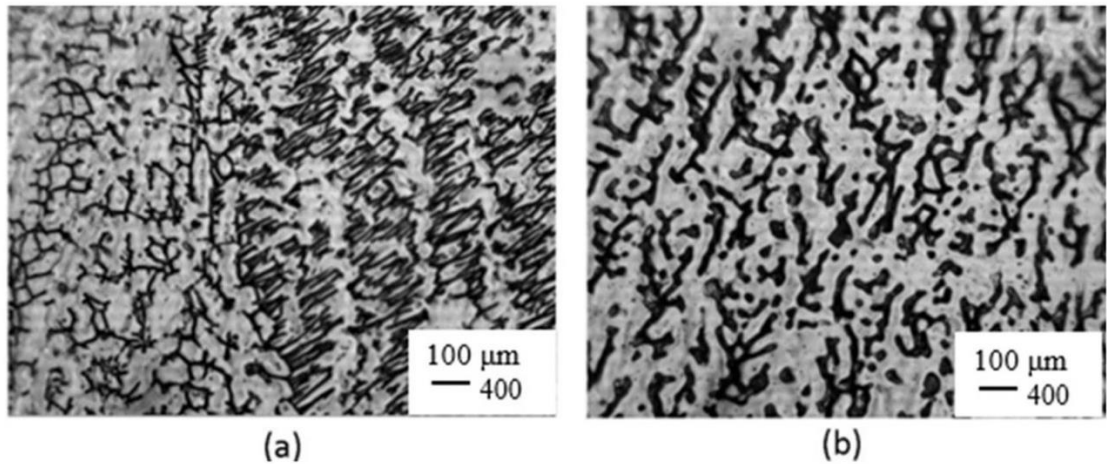


Figure 4.10. Experiment number 18 ($I=105$ A) lathy morphology (a), experiment number 27 ($I = 120$ A) vermicular morphology (b) (center point)

4.4.3. Effect of Wire Feed Speed on Microstructure

Two experiments were performed in order to investigate the effect of welding current on the microstructure of the deposited parts which are the experiments 26 and 27 with wire feed rates of 1.9 m/min and 2.1 m/min respectively. The parameters used in both experiments were $TS = 0.28$ m/min, $I = 120$ A. Figure 4.11 shows the microstructure of the two experiments. From the Fig. 4.11, it was obvious that the effect of WFS on the obtained microstructure is less than those of I and TS . However, the WFS may effect on the grain size since it leads to increasing the rate of nucleation throughout the molten metal (see Fig. 4.11(b)).

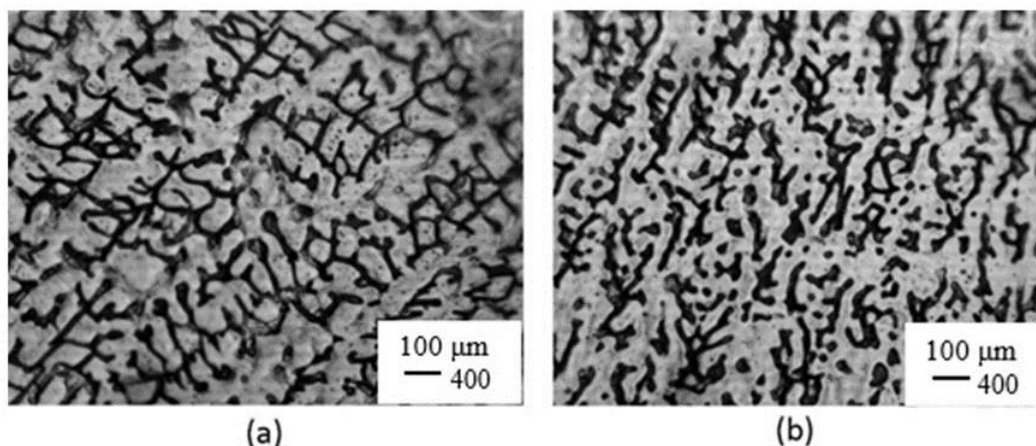


Figure 4.11. (a) Example number 26 ($WFS = 1.9$ m/min) and (b) example number 27 ($WFS = 2.1$ m/min) lathy morphology (center point)

4.5. Weld Defects

During the experiments, the two samples showed porosity because of non-isolation from the atmosphere. In addition, there was no significant weld defects present in the micro and macro analysis. During this work, examination of porosity, inclusion, lack of fusion and crack are the major mistakes. Performing the experiments in the open atmosphere led to porosity in the most specimens. Moreover, the porosity was also caused by the exposure of molten metal to oxygen, nitrogen, and hydrogen in the atmosphere.

There was no significant weld defect in micro and macro analysis. Porosities was examined in two samples. The major reason of this problem was because of the contact with atmosphere. By using argon chamber, this problem can be solved, but in this study, the argon chamber was not used because of unsuitable design of the experimental set-up.

Solid inclusions are usually expected to be a subsurface type of defect and would contain any foreign material entrapped in the deposited weld metal. The length of the deposition source with layers in the process causing solid inclusion between some samples. During this study, crack and lack of fusion and other welding errors were not observed.

4.6. Hardness

This section reports the influence of the main parameters on the hardness. The hardness was measured at the center of the wall in the cross section area at three readings were averaged. The results of the analysis of variance of the main three factors shown in Figure 4.12.

60 kg diamond cone (HRA) was used and the average value calculated by inspecting three points is shown in Table 4.1 with values ranging from 55 at maximum to 44 at minimum. Figure 4.12 shows that TS of 0.28 and WFS of 1.9 gives the highest hardness above 52. Consequently, this set of parameters was considered to obtain a high value of hardness in the application. Hardness means resistance to penetration and increasing hardness causes increasing resistance to penetration. Furthermore, mechanical properties of materials affect the hardness grain size, strain hardening,

microstructure etc. In addition, these specifications often require the results of hardness tests rather than tensile tests.

Generally, if the current increases, the hardness decreases. This means that hardness amount was affected by the amount of heat input to the deposition area. As can be seen in Figure 4.12, the highest value of hardness was achieved with the following process parameters ($I = 105$ A, $TS = 0.28$ m/min, $WFS = 1.9$ m/min).

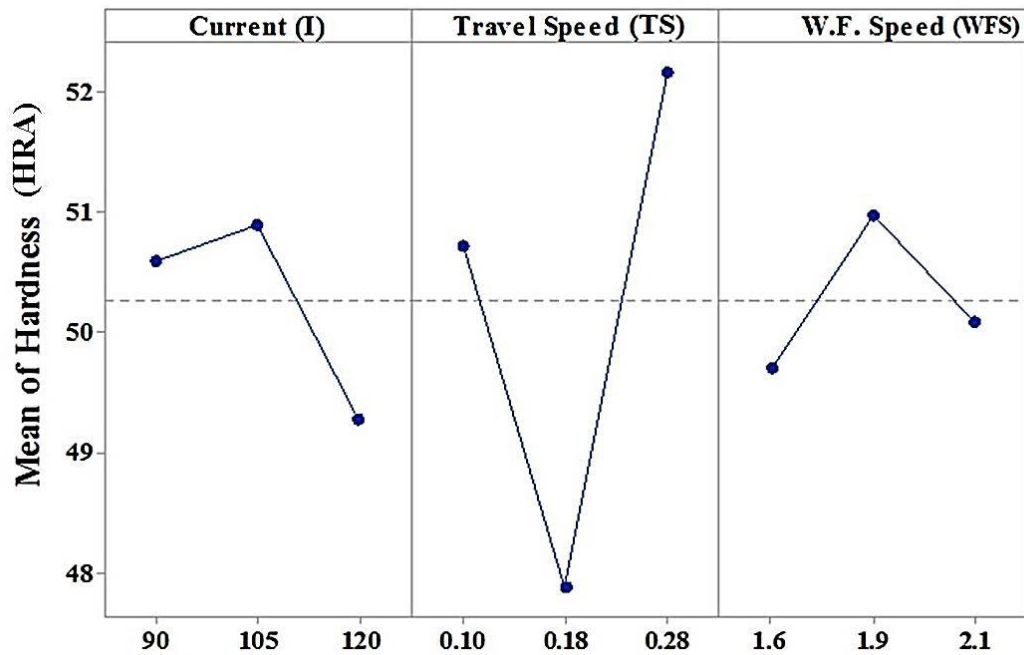


Figure 4.12. Plot illustrating the main effect of parameters on hardness

As a result, that removes quickly the generated heat from the deposition region and causing a high cooling rate and hence fast solidification rate which leads to finer size of grains and a higher hardness as observed. The results of ANOVA is shown the main parameters affecting the hardness is presented in Figure 4.12. When TS decreases from 0.1 to 0.18 m/min it can see decreases but when TS increases to 0.28 m/min it can see the hardness increases, this maybe attributed to chance errors such as wrong measurements.

CHAPTER 5

CONCLUSIONS

In this work Shaped Metal Deposition method using metal wire arc system was developed and verified to be ready to produce cylindrical metal components. Many different trials were performed to study the process and verify the process parameters.

CMD process can successfully be used to fabricate the cylindrical components made of austenite stainless steel. Several cylindrical parts were made with acceptable surface quality, zero weld defects, desirable microstructure characteristics. Stainless steel bushings with different sizes can easily be manufactured using the developed CMD machine system. The major conclusions are summarized as follows:

- Process parameters affect the shape and dimension of the weld bead. In addition, these parameters affect the thickness that results in the quality of the final surface. There is a direct relationship between input heat and process parameters, for instance, if welding arc current increases, welding speed decreases. Also, bead width of deposition is directly proportional to heat input. Layered manufacturing can be obtained by welding. In addition, bead height increases with decreasing heat input and increasing the wire feeding speed.
- On the basis of geometrical analysis results; the most suitable set of parameters which can be selected to produce cylindrical parts with stable deposition process are $I = 105 \text{ A}$, $TS = 0.1 \text{ m/min}$, and $WFS = 2.1 \text{ m/min}$. These values were determined after geometrical analysis of the produced parts for CMD machine.
- Vermicular structure was observed in the microstructure analysis of parts made with optimal parameters. Therefore, weldability and machinability better than lathe morphology. For this experiment setup, these parameters are suitable values for the geometric structure and microstructure. It may not be the same results for another application and experiment setup.

- When the current increases, the heat input to the weld pool also increases which leads to increase in the bead width. Increasing the travel speed would decrease the size of the melting pool, thus decreasing the width of the deposit. Wire feeding speed have the smallest effect on the width. The arc length is one of the most important challenges that affect the process stability, which should be maintained less than 8 mm, otherwise, the process becomes unstable and long arc way lead to destroying the deposition walls.
- The current ratio effects significantly on the morphology and final microstructure of the deposited parts.
- Macro studies did not show the welding faults on the connection between the layers. There was no significant weld defect noticeable in both micro and macro analysis.
- The austenite skeletal (vermicular) ferrite is observed when cooling rate is moderate and the C_{req}/Ni_{eq} ratio is low within FA range. In addition, high cooling rate and increasing ratio of C_{req}/Ni_{eq} would result with austenite lathy ferrite. The place of vermicular morphology creates lathy morphology owing to limited dispersion during austenite ferrite transformation.
- According to the micro analysis results, vermicular and lathy ferrite morphologies were observed. For some samples vermicular ferrite content is greater than the others. Due to fast cooling. As the results of the investigation, TS and I value had effect on microstructure, however, changes in the value of WFS did not have any significant effect on the microstructure.
- As a result of the experiments, cooling times were not calculated. Ambient conditions could be affect cooling time. So, results may vary in different experimental setup.
- At the beginning of the experiment, differences in microstructure of the first layer have been made to prevent by heating base plate.
- According to the hardness results, as the current increases, the hardness would decrease. This means that hardness of the sample was affected by the amount of heat input to the deposition area. The results of ANOVA is shown the main parameters affecting the hardness is presented in Figure 4.12. When TS decreases from 0.1 to 0.18 m/min it can see decreases but when TS increases to 0.28 m/min it can see the hardness increases, this maybe attributed to chane errors such as wrong measurements.

- The forging and casting processes are used to produce near net shaped components, which usually at the finished features by machining processes. So less raw material is used, therefore, less machining is necessary and less coolant, tooling and energy use. It has been known that casting and forging processes required a large amount of energy to create. Also, these techniques have process constraints; this means that they may be unable to produce very near shaped components. These methods are not flexible since they are expensive and time-consuming in molds and dies preparation.
- Consequently, all the tests and examination yielded that this method would be an alternative manufacturing process for some critical parts and even ordinary parts to be used in different industries.

5.1. Future Work

A process window can be generated for the selected materials by conducting workshop experiments and showing the effects of the process parameters.

Thermal analysis of the deposited materials can be modeled using finite element method.

Thermal residual stresses and thermal defects can be measured after deposition.

REFERENCES

- [1] Wang H., Kovacevic R. (2001). Rapid prototyping based on variable polarity gas tungsten arc welding for a 5356 aluminium alloy. *Proc ImechE, J Engineering manufacture*, **215-B**, 1519 - 1527.
- [2] Mehnen J., Ding J., Lockett H., Kazanas P. (2010). Design for Wire and Arc Additive Layer Manufacture. *Proceedings of the 20th CIRP Design Conference*, 721 - 727.
- [3] Baufeld B., Van der Biest O., Gault R. (2010). Additive manufacturing of Ti6Al4V components by shaped metal deposition: Microstructure and mechanical properties. *Materials and Design*, **31**, 106 - 111.
- [4] Baufeld B., Gault R., Van der Biest O. (2009). Microstructure of Ti-6Al-4V specimens produced by shaped metal deposition. *Material Research*, **100/11**, 1536 - 1542.
- [5] Baufeld B., Van der Biest O., Gault R., Ridgway K. (2011). Manufacturing Ti6Al4V components by shaped metal deposition: Microstructure and mechanical Properties. *IOP Conference Series, Material Science and Engineering*, **26/1**.
- [6] Martina F., Mehnen J., Williams S. W., Colegrove P., Wang F. (2011). Investigation of the benefits of plasma deposition for the additive layer manufacturing of Ti-6Al-4V. *Material processing technology*, **212**, 1377 - 1386.
- [7] ASTM, American Society for Testing and Materials (1998). Standard test method for tensile properties of thin plastic sheeting. D882-97, West Conshohocken, PA.
- [8] Frazier W. E. (2014). Metal Additive Manufacturing: A review. *Mater Engineering, and Performance*, **23/6**, 1917 - 1928.
- [9] Baufeld B., Van der Biest O. (2009). Mechanical properties of Ti-6Al-4V specimens produced by shaped metal deposition. *Science, and technology of advanced materials*, **10**, 10.
- [10] Escobar-Palafox G., Gault R., Ridgway K. (2011). Preliminary empirical models for predicting shrinkage, part geometry and metallurgical aspects of Ti-6Al-4V shaped metal deposition builds. *Trends in aerospace manufacturing international conference*, **26**.
- [11] Yilmaz O., Almusawi A. R. J., Uglu A. A., Keskin O. O. (2015). Design, Construction, and Controlling of A Shaped Metal Deposition Machine Using Arc Metal -Wire System. *8th International Conference and Exhibition on Design and Production of Machines and Dies/molds*, 235 - 244.

- [12] Clark, D., Bache M. R., Whittaker M. T. (2008). Shaped metal deposition of A nickel for aero engine applications. *Material Processing Technology*, **203**, 439 - 448.
- [13] Brandl E., Michailov V., Viehweger B., Leyens C. (2011). Deposition of Ti-6Al-4V using laser and wire, part II: Hardness and dimensions of single beads. *Surface and Coating Technology*, **206**, 1130 - 1141.
- [14] Qian Y. P., Huang J. H., Zhang H. O., Wang G. L. (2008). Direct rapid high-temperature alloy prototyping by hybrid plasma-laser technology. *Material Processing Technology*, **208**, 99 - 104.
- [15] Dinda G. P., Dasgupta A. K., Mazumder J. (2009). Laser-aided direct metal deposition of Inconel 625 superalloy: Microstructural evolution and thermal stability. *Material Science and Engineering*, **509-A**, 98 - 104
- [16] Mahamood R. M., Akinlabi E. T., Shukla M., Pityana S. (2013). Laser metal deposition of Ti6Al4V: A study on the effect of laser power on microstructure and microhardness. *Proceedings of the International MultiConference of Engineers and Computer Scientists*, **2**, 978 - 988.
- [17] Cheng B., Chou K. (2014). Thermal stresses associated with part overhang geometry in electron beam additive manufacturing: process parameter effects. *International Manufacturing Science and Engineering Conference*, **4063**.
- [18] Antonysamy A. A. (2012). Microstructure, Texture and Mechanical Property Evolution during Additive Manufacturing of Ti6Al4V Alloy for Aerospace Applications. University of Manchester of The Faculty of Engineering and Physical Sciences.
- [19] Agilent de Saracibar C., Lundbäck A., Chiumenti M., Cervera M. (2014). Shaped metal deposition processes. *Encyclopedia of Thermal Stresses*, 4347 - 4355.
- [20] Hoye N. P., Appel E. C., Cuiuri D., Li H. (2013). Characterisation of metal deposition during additive manufacturing of Ti-6Al-4V by arc-wire methods. *Proceeding of the 24th annual international solid freeform fabrication symposium*, 1015 - 1023.
- [21] Xiong X., Zhang H., Wang G. (2008). Metal direct prototyping by using hybrid plasma deposition and milling. *Material processing technology*, **209**, 124 -130.
- [22] Escobar-Palafox G., Gault R., and Ridgway K. (2011). Robotic manufacturing by shaped metal deposition: State of the art. *Industrial robot: An International journal*, **38/6**: 622 - 628.
- [23] Srivatsan T. S., Sudarshan T. S.(2016). Additive Manufacturing Innovations, Advances, and Applications. CRC PressTaylor & Francis Group, LLC.
- [24] Baufeld B., Brandl E., Van der Biest O. (2011). Wire based additive layer manufacturing: Comparison of microstructure and mechanical properties of Ti-6Al-4V components fabricated by laser-beam deposition and shaped metal deposition. *Material technology*, **211**, 1146 - 1158.
- [25] Brandl E., Baufeld B., Leyens C., Gault R. (2010). Additive manufactured Ti-6Al-4V using welding wire: comparison of laser and arc beam deposition and evaluation with respect to aerospace material specifications. *Physics Procedia*, **5**, 595 - 606.

- [26] Yilmaz O., Ugla A.A. (2016). Shaped metal deposition technique in additive manufacturing: A review. *Proc IMechE Part B: J Engineering Manufacturing*, Published online, April 2016, DOI: 10.1177/0954405416640181.
- [27] Yilmaz O., Ugla A.A. (2016). Microstructure characterization of SS308LSi components manufactured by GTAW-based additive manufacturing: shaped metal deposition using pulsed current arc. *Int. J. Adv. Manuf. Technol*, Published online, June 2016, DOI 10.1007/s00170-016-9053-y
- [28] RAPOLAC Project home page. <http://www.rapolac.eu>
- [29] Skiba T., Baufeld B., Van Der Biest O. (2009). Microstructure and mechanical properties of stainless steel component manufacturing by shaped metal deposition. *ISIJ International*, **49**, 1588 - 1591
- [30] Heralić A., Christiansson A. K., Hurtig K. (2008). Control design for automation of robotized laser metal-wire deposition. *17th world congress the international federation of automatic control*.
- [31] Bonaccorso F., Bruno C., Cantelli L. (2009). Control of a shaped metal deposition process. *Proceedings of the 4th international scientific conference on physics and control (PHYSCON)*.
- [32] Zhang Y. M., Li P., Chen Y., Male A. T. (2002). Automated system for welding-based rapid prototyping. *Mechatronics*, **12**, 37 - 53.
- [33] Mirshekari G. R., Tavakoli E., Atapour M., Sadeghian B. (2014). Microstructure and corrosion behavior of multipass gas tungsten arc welded 304L stainless steel. *Material, and design*, **55**, 905 - 911.
- [34] Li K., Li D., Liu D., Guangyu P., Sun L. (2015). Microstructure evolution and mechanical properties of multiple-layer laser cladding coating of 308L stainless steel. *Applied surface science*, **340**, 143 - 150.
- [35] Folkhard E. (1988). *Welding Metallurgy of Stainless Steels*. 1st edition, Springer-Verlag/Wien.
- [36] Lippold J. C., Kotecki D. J. (2005). *Welding metallurgy and weldability of stainless steels*. John Wiley & Sons, Inc., Hoboken, New Jersey.
- [37] Lippold J. C., Savage W. F. (1980). Solidification of austenitic stainless steel weldment: Part 2-The effect of alloy composition on ferrite morphology. *Welding research supplement*.
- [38] Austenitic stainless steels (2008). *Stainless steel for design engineers*. Available at www.asminternational.com.
- [39] DIN. Deutsches Institut für Normung. Burggrafenstrasse 6 10787 Berlin Germany.
- [40] Budynas, R. G., Nisbett, J. K., & Shigley, J. E. (2011). *Shigley's mechanical engineering design*. New York: McGraw-Hill.
- [41] Box, G.E.; Hunter, J.S.; Hunter, W.G. (2005). *Statistics for Experimenters: Design, Innovation, and Discovery*. 2nd Edition. Wiley.
- [42] Tatsumi N., Harano K., Ito T., Sumiya H. (2015). Polishing mechanism and surface damage analysis of type Iia single crystal diamond processed by mechanical and chemical polishing methods. *Diamond & related materials*.

[43] ASM, American Society of Metals (1973). Metals Handbook - Metallography, structure and phase diagrams. 8th edition, 27-12046, Ohio.

[44] Peckner D., Bernstein I. M. (1977). Handbook of stainless steel, McGraw-Hill Book Company. 76-54266, The United States of America.

[45] G. Dieter (1986). Mechanical Metallurgy. Mc Graw Hill, The United States of America.



APPENDIX

Appendix A

Welding Machine Technical Specifications

The Invertec V320-T AC/DC (see Figure A.1) are industrial TIG welding machines designed and manufactured using the latest inverter digital technology enabling the machines to perform at high outputs: respectively 320A at 35% duty cycle.



Figure A.1. TIG welding machine

The controller provides all the features you would expect from professional AC/DC TIG inverter welding machines combined with a user-friendly layout. The variable frequency control allows the welder to adjust the arc focus to suit the application.

A standard feature is the adjustable cleaning and penetration facility, used to gain the ideal balance between cleaning the aluminum surface of oxide and the penetration of the weld. The machines operate using a square wave AC form as standard but can be set to an alternative waveform dependent on the welder's needs. Adjustable starting current is also available on these machines.

The machines are supplied air-cooled as standard, however, they can be easily converted to water-cooled .

Table A1. TIG welding machine specification

Technical Specifications					
Product	Item Number	Primary Voltage	Fuse Size	Weight	Dimensions (HxWxD)
V320-T AC/DC	K12046-1	230/400V/3/50- 60 Hz	25A	33 Kg	432x280x622
Product	Item Number	Flow Rate	Tank Capacity	Weight	Dimensions (HxWxD)
Cool Arc® 34	K12047-1	2.5 Liters/min.	5L	16 Kg	256x280x622

